Water Research 185 (2020) 116136

Contents lists available at ScienceDirect

Water Research

journal homepage: www.elsevier.com/locate/watres

A novel peroxymonosulfate (PMS)-enhanced iron coagulation process for simultaneous removal of trace organic pollutants in water

Yu Wang, Tao Pan, Yafei Yu, Yang Wu, Yanheng Pan, Xin Yang*

School of Environmental Science and Engineering, Guangdong Provincial Key Laboratory of Environmental Pollution Control and Remediation Technology, Sun Yat-sen University, Guangzhou, 510275, China

ARTICLE INFO

Article history:
Received 27 March 2020
Received in revised form
3 June 2020
Accepted 30 June 2020
Available online 6 August 2020

Keywords:
Peroxymonosulfate (PMS)
Coagulation
Trace organic compounds
Carbamazepine
Sulfate radical
Water treatment

ABSTRACT

Conventional coagulation process is not effective to eliminate trace organic compounds (TrOCs). This study proposed a novel peroxomonosulfate (PMS) amended iron coagulation process and found its effectiveness in eliminating TrOCs in synthetic and natural waters. In synthetic waters containing hydroquinone (HQ) or benzoquinone (BQ), Fe(III)/PMS effectively degraded carbamazepine (CBZ), a representative of resistant TrOCs. The step of reduction of Fe(III) to form Fe(II) governed the degradation rate of CBZ as PMS activation by Fe(II) was the dominant reaction to generate $SO_4^{\bullet-}$, which was the major reactive oxidant in the system. Meanwhile, HQ was quickly transformed to BQ in the Fe(III)/PMS system and BQ acted as an electron shuttle to induce Fe(III)/Fe(II) redox cycle and accelerate PMS activation. Natural organic matter (NOM) bearing phenolic and quinone moieties played similar roles as HQ and BQ and fast CBZ degradation was also observed. Finally, two surface waters spiked CBZ were subjected to bench-scale experimentation to simulate coagulation/flocculation/sedimentation processes in water treatment plants. Compared to the conventional iron coagulation process, the PMS-amended iron coagulation process increased the removal percentage of CBZ by 50%–80%. Overall, this study demonstrates that PMS enhanced iron coagulation is a promising process for the abatement of TrOCs in water treatment.

1. Introduction

Trace organic compounds (TrOCs), such as pharsmaceutical and personal care products (PPCPs) and endocrine disrupting chemicals (EDCs), have been frequently detected in surface waters at ng/-μg/L levels (Padhye et al., 2014; Zhang et al., 2015). The conventional water treatment processes, such as coagulation, sedimentation and filtration units, were not very effective in removing TrOCs (Huerta-Fontela et al., 2011; Westerhoff et al., 2005). Chlorination can remove some TrOCs bearing phenolic, amine and aniline groups (Huerta-Fontela et al., 2011; Westerhoff et al., 2005). A variety group of TrOCs were thus still detected in the finished drinking water (Gaffney et al., 2015; Loraine and Pettigrove, 2006). Considering that some of TrOCs have been linked to adverse health and ecological effects (Bruce et al., 2010; Liu et al., 2020), improving the degradation efficiency of TrOCs in drinking water treatment processes is still urgently needed.

Activated persulfate, including peroxomonosulfate (PMS) and peroxydisulfate (PDS), has been widely used to eliminate various TrOCs, taking advantage of sulfate ($SO_4^{\bullet-}$) or hydroxyl ($HO^{\bullet}$) radicals (Ghanbari and Moradi, 2017; Lee et al., 2020; Cheng et al., 2020). Among the activators used, ferrous iron (Fe(II)) was commonly adopted. Parallel to the Fenton reaction, this process proceeds through one-electron reduction of the -O-O- bond to produce sulfate radical ($SO_4^{\bullet-}$) (Eqs. (1) and (2)) (Kim et al., 2018; Zou et al., 2013). However, due to the limitation of slow transformation rate from the formed Fe(III) back to Fe(II), the degradation of contaminants was quickly inhibited and resulted in incomplete degradation. To alleviate the drawbacks, multiple antioxidants such as hydroxylamine and natural polyphenols have been proposed to assist the redox cycling of Fe(III)/Fe(II) (Pan et al., 2020; Zou et al., 2013). In addition to Fe(II), recent studies indicated that naturally occurring quinones can also activate persulfate. For example, 1,4-benzoquinone (BQ) can effectively decompose PDS to $SO_4^{\bullet-}$ for 2,4,4′-trichlorobiphenyl (PCB 28) degradation (Fang et al., 2013). The activation of PMS by BQ, however, produced singlet oxygen ($^1O_2$), not $SO_4^{\bullet-}$ (Ahmad et al., 2013). Despite of many researches on

* Corresponding author.
E-mail address: yangx36@mail.sysu.edu.cn (X. Yang).

https://doi.org/10.1016/j.watres.2020.116136
0043-1354/

PMS/PDS activation by Fe(II) or phenols/quinones, the application of these processes in drinking water treatment is still questionable, partially because the addition of Fe(II) or other activators may lead to secondary pollution or bring problems for the subsequent treatment steps, e.g. disinfection.

$$Fe(II) + H-O-O-SO_3^- \rightarrow Fe(III) + SO_4^{\bullet -} \quad k = 3.0 \times 10^4\ M^{-1}\ s^{-1} \tag{1}$$

$$Fe(II) + {}^-_3O\,S-O-O-SO_3^- \rightarrow Fe(III) + SO_4^{2-} + SO_4^{\bullet -} \quad k = 2.0 \times 10^1\ M^{-1}\ s^{-1} \tag{2}$$

In water treatment, ferric (Fe(III)) salts including ferric chloride and ferric sulfate are commonly used as coagulants to remove suspended solids (SS) and some natural organic matter (NOM) (Matilainen et al., 2010; Vik and Eikebrokk, 1988). NOM is ubiquitous in natural waters and contains numerous phenolic and quinone moieties (Aeschbacher et al., 2012; Cory and McKnight, 2005). Previous results show that the phenolic and quinone moieties are involved in the redox transformation of iron. For example, Garg and coworkers found that hydroquinone and/or semiquinone-type species present in NOM can reduce Fe(III) to Fe(II) in natural waters (Garg et al., 2015). For benzoquinone, although it cannot directly reduce Fe(III), it can undergo self-redox cycling to produce semiquinone or hydroquinone to interact with Fe(III) (Song and Buettner, 2010). Therefore, we suspect that if PMS is added to the coagulation process, these redox active moieties (phenols and quinones) present in NOM might assist in PMS activation. Possible reactions include (i) activation of PMS by benzoquinone or semiquinone moieties (Ahmad et al., 2013; Fang et al., 2013; Zhou et al., 2015); (2) activation of PMS by Fe(II) formed from reduction of Fe(III) (Anipsitakis and Dionysiou, 2004); (3) regeneration of Fe(II) via hydroquinone/quinone redox reactions (Jiang et al., 2015). An understanding of these reactions is thus important for the potential application of PMS-amended iron coagulation for TrOCs degradation.

As such, the aim of this study is to verify whether Fe(III)/quinone and Fe(III)/hydroquinone interactions can be used to activate PMS for TrOC degradation and whether the PMS amended iron coagulation is feasible for TrOCs degradation for natural waters. Carbamazepine (CBZ) was chosen as the target compound, due to its prevalence in surface waters and resistance to common oxidants (e.g., chlorine, chlorine dioxide, hydrogen peroxide and PMS/PDS). In some tests, caffeine, ibuprofen, atrazine are also included as they are also known to be resistant by conventional water treatment processes. Benzoquinone (BQ) and hydroquinone (HQ) were used as representatives of oxidized and reduced quinones, respectively because of their simple structures and well-studied reactions with Fe(III). Surface water samples were used for coagulation/flocculation/sedimentation treatment processes. The results from this study are inspiring and provide a potential application of upgrading the traditional coagulation process to bear advanced oxidation functions for TrOCs removal.

2. Materials and methods

2.1. Chemicals

1,4-Benzoquinone (BQ, ≥ 98%), 2-methylhydroquinone (MHQ, 99%), 2-chlorohydroquinone (CHQ, 85%), 2-chloro-1,4-benzoquinone (CBQ, 95%), 2-methyl-1,4-benzoquinone (MBQ, 98%), Rose Bengal (RB, 95%), methyl phenyl sulfoxide (PMSO, ≥ 97%), methyl phenyl sulfone ($PMSO_2$, ≥98%), 5,5-dimethyl-1-pyrroline N-oxide (DMPO, ≥ 98%), 2,2,6,6-tetramethyl-4-piperidinol (TEMP, 98%), carbamazepine (CBZ, ≥ 98%), nitrobenzene (NB, ≥ 99%), benzoic acid (BA, ≥ 99.5%), caffeine (≥98%), ibuprofen (≥98%) and atrazine (≥98%) were purchased from Sigma-Aldrich (USA). $Fe_2(SO_4)_3{\bullet}xH_2O$, $FeCl_3{\bullet}6H_2O$ (≥99%), and $FeSO_4$ (≥98%) were obtained from Sinopharm Chemical Reagent Co., Ltd (Shanghai, China). Peroxymonosulfate ($KHSO_5{\cdot}0.5\ KHSO_4{\cdot}0.5K_2SO_4$, 4.5% active oxygen), 1,4-hydroquinone (HQ, 99%), 3-(2-Pyridyl)-5,6-diphenyl-1,2,4-triazine-4′,4″-disulfonic acid sodium salt (abbreviated as ferrozine, 97%) and superoxide dismutase (SOD, 2×10^4 units/mg) were purchased from Macklin Biochemical Co., Ltd (Shanghai, China). Methanol (MeOH), tert-butyl alcohol (TBA) were supplied by ANPLE Laboratory Technologies (China). Suwannee River Fulvic acid (SRFA, 2S101F) was obtained from International Humic Substances Society (IHSS). Two surface water samples were collected from Beijiang River and Pearl River in Guangdong, China, and stored at 4 °C in dark until use. The characteristics of the water samples are summarized in Table S1.

2.2. Experimental procedures

Degradation experiments involving quinone/Fe(III)/PMS and SRFA/Fe(III)/PMS processes were conducted in 100 mL Erlenmeyer flasks under magnetic stirring at 25 (±1) °C. A baseline condition was that the concentrations of CBZ, Fe(III), PMS and HQ (or BQ) were fixed at 2 μM, 0.05 mM, 0.5 mM and 0.1 mM, respectively. In a typical run, BQ (or HQ), Fe(III), and CBZ solutions were mixed first, then PMS was quickly added to initiate the reaction. No pH adjustment was conducted before and during the reaction. After reaction for 1, 3, 5, 8, 10, 15, 30, and 60 min, 1.0 mL of the sample was sampled and mixed with 100 μL of 100 mM $Na_2S_2O_3$ to terminate the reaction. Then, the samples were filtered with 0.45 μm glass fiber membrane (Jinteng, China) before analysis. Control experiments were conducted to evaluate the degradation of CBZ by PMS alone, Fe(III)/PMS, BQ/PMS and HQ/PMS processes. To evaluate the performance of BQ/Fe(III)/PMS process in the degradation of other TrOCs, BA, NB, caffeine, ibuprofen, and atrazine were added separately at 2 μM as the target compound. To investigate the role of dissolved oxygen (DO) in the experimental system, the solutions used were sparged with argon for 4 h prior to experiments. Sparging was continued during the reaction period to keep the concentration of DO less than 0.1 mg/L. In certain tests, NB and BA were added as probe compounds to determine the steady-state concentrations of $HO^{\bullet}$ and $SO_4^{\bullet -}$, respectively (see details in Text S1). In some tests, NOM was used to replace HQ or BQ. Varied concentrations of SRFA (1 mgC/L, 2.5 mgC/L, and 5 mgC/L) were added to the Fe(III)/PMS process to mediate CBZ degradation. To further confirm the contribution of $HO^{\bullet}$ and $SO_4^{\bullet -}$ in CBZ degradation in SRFA/Fe(III)/PMS process, scavenging experiments were conducted by adding 10 mM MeOH or TBA (the molar alcohol/CBZ ratio was 1000:1) to the reaction system. All the degradation experiments were conducted in duplicate.

Two surface water samples from Beijiang River and Pearl River were used for ferric coagulation experiments, which were conducted as jar tests using a 6-place programmable multiple stirrer (ZR4-6, Zhongrun Water Industry Technology Development Co., Ltd.) with 1-L square plastic floc jars. The two water samples were both treated by PMS, Fe(III) and Fe(III)+PMS coagulation processes. Specifically, 0.4 μmol of CBZ was spiked to 0.8 L source water. Then, 6 mL of Fe(III) solution (26.7 mM) and 2 mL of PMS solution (0.4 mM) were added simultaneously to the water samples and the rapid mixing step immediately started. The final concentrations of CBZ, Fe(III) and PMS in this process were 0.5 μM, 0.2 mM, and 1 mM, respectively. The mixing procedures were conducted as follows: 1 min of rapid mixing at 200 rpm, 30 min of flocculation at

30 rpm, and 90 min of settling time. Control experiments with Fe(III) or PMS alone were also conducted. After reaction for 5, 15, 30, 60, 90, and 120 min, 1 mL of supernatant was withdrawn and mixed with 100 μL of 100 mM $Na_2S_2O_3$ to stop the reaction. The filtrates were subjected to analysis on high performance liquid chromatography (HPLC) after filtration with 0.45 μm filters. To investigate the effect of $[PMS]_0$ on CBZ degradation, different dosages of PMS (0.2, 0.5, and 1 mM) were added during ferric coagulation of Beijiang River water. All the coagulation treatments were performed in duplicate.

2.3. Analytical methods

The concentrations of BQ, HQ and the other organic compounds were analyzed using a UltiMate™ 3000 HPLC system (Thermo Fisher Scientific Inc., USA) equipped with a diode array detector and a Syncronis C18 column (4.6 × 250 mm, 5 μm, Thermo Fisher). Details of the mobile phases and detected wavelengths were summarized in Table S2. PMS was determined using the iodometric titration method on a UV-1800 spectrophotometer (Shimadzu, Japan) at a wavelength of 352 nm (Wacławek et al., 2015). Fe(II) was measured by the ferrozine colorimetric method (λ_{max} = 562 nm) which is shown in previous study (Stookey, 1970).

An electron paramagnetic resonance (EPR) spectrometer (Bruker A300-10/12, Germany) was employed to detect the ROS by reacting with 100 mM DMPO or TEMP. The samples were transferred into a capillary tube and analyzed under the following conditions: microwave power = 20 mW, microwave frequency = 9.829 GHz, center field = 3507 G, sweep width = 100 G, and modulation frequency = 100 kHz.

3. Results and discussion

3.1. Degradation of CBZ in BQ/Fe(III)/PMS and HQ/Fe(III)/PMS processes

The degradation kinetics of CBZ in different PMS-based oxidation processes are shown in Fig. 1. CBZ can't be degraded by PMS alone. Less than 8% CBZ was degraded in HQ/PMS and Fe(III)/PMS processes within 60 min. About 20% CBZ was degraded in BQ/Fe(III) process after 60 min. However, when BQ was added to Fe(III)/PMS system, the degradation of CBZ was significantly accelerated and showed a two-stage decay kinetics. About 20% CBZ was degraded in the initial 1 min (the first sampling point), after which the degradation proceeded moderately, reaching 99% after 60 min. In comparison, the degradation of CBZ was much faster in HQ/Fe(III)/PMS process, i.e., almost all CBZ was degraded within 8 min. Such faster degradation rate can be attributed to the high reactivity of HQ toward Fe(III) (2.4×10^6 M^{-1} s^{-1}) (Jiang et al., 2015), which generates Fe(II). As shown in Fig. S1, PMS activation by Fe(II) (50 μM) was very effective to eliminate CBZ and about 90% of CBZ was degraded in 1 min. Afterwards, the degradation of CBZ almost stopped, due to the limitation of Fe(III) transformation back to Fe(II), which is similar to the case in Fenton reaction. Except BQ and HQ, the effects of other substituted quinones were also examined. The addition of CHQ, CBQ or MHQ in Fe(III)/PMS system resulted in complete degradation of CBZ after 8 min and 89% CBZ was degraded in MBQ amended Fe(III)/PMS system in the same period (Fig. S2). The results suggest that quinone and/or hydroquinone moieties can effectively mediate Fe(III) for PMS activation and thus promote CBZ degradation.

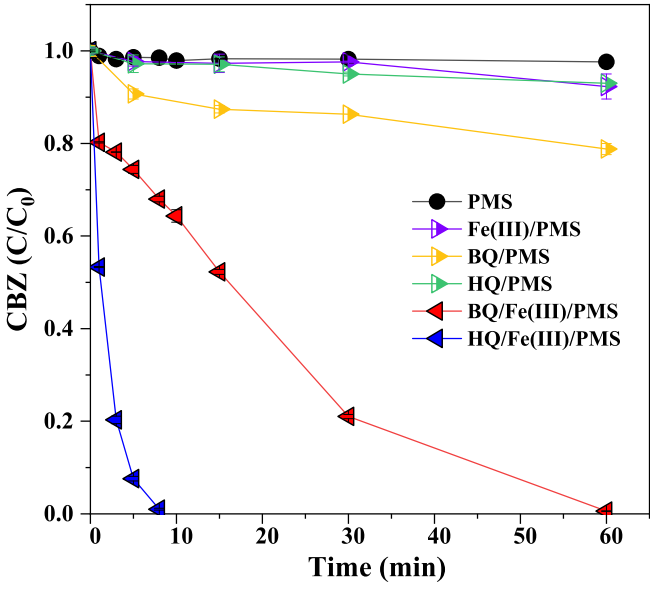

Fig. 1. Degradation kinetics of CBZ in different reaction systems. (CBZ = 2 μM, Fe(III) = 0.05 mM, HQ = BQ = 0.1 mM, PMS = 0.5 mM).

3.2. Identification the roles of reactive oxidants

A series of experiments were conducted to further explore the roles of reactive species in BQ/Fe(III)/PMS systems by the use of probe compounds, quenchers and EPR spectroscopy methods. Self-decomposition of PMS or BQ-catalyzed PMS activation was reported to generate $^1O_2$ (Li et al., 2018; Zhou et al., 2015). To verify the generation of $^1O_2$ in BQ/Fe(III)/PMS process, TEMP was used as the trapping agent in EPR spectroscopy. As shown in Fig. S3, a typical 3-fold characteristic peak of the TEMP-$^1O_2$ adduct (α = 16.9 G) with an intensity ratio of 1:1:1 (Sun et al., 2019) was observed in solution containing PMS alone, primarily due to its self-decomposition. Although higher TEPM-$^1O_2$ signal was observed in BQ/Fe(III)/PMS process, it should be noted that its intensity was similar as that in BQ/PMS, whereas the latter showed negligible CBZ degradation (Fig. 1). Moreover, the reactivity of $^1O_2$ with CBZ was low, which was determined to be 2.57×10^5 M^{-1} s^{-1} in this study (details in Text S2). The results indicated that $^1O_2$ played a negligible role in CBZ degradation.

The EPR results showed a typical DMPO-SO_4 signal (a_N = 13.2 G, a_H = 9.6 G, a_H = 1.48 G and a_H = 0.78 G) (Fang et al., 2013) in quinone/Fe(III)/PMS process (Fig. 2a), indicating the generation of $SO_4^{\bullet-}$ in this process. The peak intensity of DMPO-SO_4 in BQ/Fe(III)/PMS process was slightly lower than that in HQ/Fe(III)/PMS, which was consistent with the difference in CBZ degradation observed in Fig. 1. The signal of DMPO-OH ($a_N = a_H$ = 14.9 G) was too small to observe in BQ/Fe(III)/PMS and HQ/Fe(III)/PMS processes. To further explore the role of $SO_4^{\bullet-}$ and $HO^{\bullet}$ in CBZ degradation, BA and NB were added as probe compounds. As shown in Table S3, BA reacted both with $SO_4^{\bullet-}$ ($k = 1.2 \times 10^9$ M^{-1} s^{-1}) and $HO^{\bullet}$ ($k = 4.2 \times 10^9$ M^{-1} s^{-1}) (Neta et al., 1977), and NB mainly reacted with $HO^{\bullet}$ ($k = 3.9 \times 10^9$ M^{-1} s^{-1}), but barely with $SO_4^{\bullet-}$ ($k < 1 \times 10^6$ M^{-1} s^{-1}) (Buxton et al., 1988). As shown in Fig. 2b, insignificant amount of NB was degraded after 60-min reaction in the BQ/Fe(III)/PMS system, whereas BA was degraded by 96% in the same period. Clearly, $SO_4^{\bullet-}$, but not $HO^{\bullet}$ was the dominant specie in the BQ/Fe(III)/PMS system. Quenching experiments were also conducted by using BA, NB and MeOH. In this study, the addition of 0.4 mM BA would completely quench almost all the generated $SO_4^{\bullet-}$ ($(k_{SO4\bullet-,\ BA} \times [BA])/(k_{SO4\bullet-,\ BA} \times [BA] + k_{SO4\bullet-,\ CBZ} \times [CBZ]) = 99.2\%$) and $HO^{\bullet}$ ($(k_{HO\bullet,\ BA} \times [BA])/(k_{HO\bullet,\ BA} \times [BA] + k_{HO\bullet,\ CBZ} \times [CBZ]) = 99\%$), while 0.5 mM NB will only quench all the $HO^{\bullet}$ ($(k_{HO\bullet,\ NB} \times [NB])/(k_{HO\bullet,\ NB} \times [NB] + k_{HO\bullet,}$

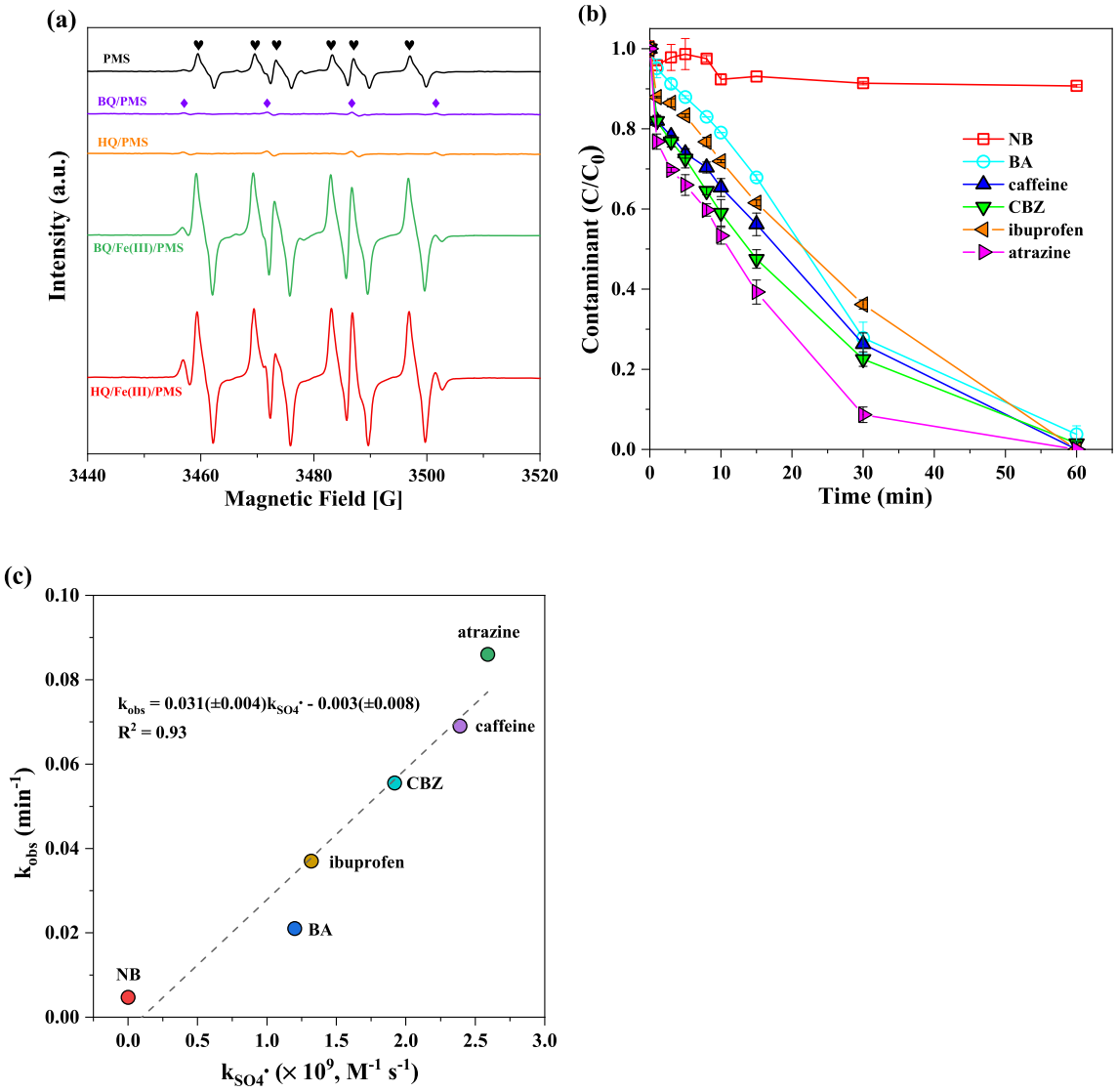

Fig. 2. (a) EPR spectra for different reaction processes (♥ DMPO-SO_4, ◆DMPO-OH). (DMPO = 100 mM, PMS = 11.25 mM, BQ = HQ = 2.25 mM, Fe(III) = 1.125 mM); (b) Selective degradation of different TrOCs by BQ/Fe(III)/PMS process. (TrOCs = 2 μM); (c) The relationship between TrOC degradation rates and their reaction rate constants with $SO_4^{\bullet-}$.

$_{CBZ}$ × [CBZ]) = 99.1%). As shown in Fig. S4, the degradation of CBZ after 60 min was reduced by only 13% in the presence of 0.5 mM NB, while it was markedly retarded and almost terminated when 0.4 mM BA was added. Meanwhile, the addition of 250 mM MeOH (($k_{SO4\bullet-,\ MeOH}$ × [MeOH])/($k_{SO4\bullet-,\ MeOH}$ × [MeOH] + $k_{SO4\bullet-,\ CBZ}$ × [CBZ]) > 99.9%) also greatly inhibited CBZ degradation (Fig. S4). Besides CBZ, atrazine, caffeine, and ibuprofen were also selected as the target compounds to evaluate the BQ/Fe(III)/PMS process. These compounds are refractory to $^1O_2$ oxidation (Zhu et al., 2019), but can be degraded by $SO_4^{\bullet-}$ (~10^9 M^{-1} s^{-1}) (Table S3). As shown in Fig. 2b, atrazine, caffeine, and ibuprofen were completed degraded within 60 min. However, in the presence of 0.4 mM BA, no significant degradation was observed for these TrOCs (Fig. S5). Further, TrOC decay within the first 30 min was fitted with pseudo-first-order kinetic model ($\ln([TrOC]_t/[TrOC]_0) = -k_{obs}t$), then the correlation of k_{obs} and the rate constant of TrOC with $SO_4^{\bullet-}$ ($k_{SO4\bullet-}$) was plotted. A good linear relationship ($R^2 = 0.93$) was observed between k_{obs} and $k_{SO4\bullet-}$ (Fig. 2c), again suggesting that $SO_4^{\bullet-}$ was mainly responsible for TrOC degradation. Additionally, the formation of high-valent iron species (e.g. (Fe(IV) and Fe(V)) was not observed from the experimental results of the distinct transformation of methyl phenyl sulfoxide (PMSO) to methyl phenyl sulfone ($PMSO_2$) (details in Text S3 and Fig. S6). Thus, the above results provide solid evidence that BQ/Fe(III)/PMS process is a $SO_4^{\bullet-}$-dominated process. It should be noted that HQ/Fe(III)/PMS process is also dominated by $SO_4^{\bullet-}$ because HQ is quickly converted to BQ in the system (<1 min) with details discussed below.

3.3. The redox reactions of BQ/HQ, Fe(II)/Fe(III) and the formation of $SO_4^{\bullet-}$

The concentrations of BQ and HQ were also tracked in the reaction system (Figs. 3a-1). Approximately 4.7 μM of HQ existed in the BQ solution (100 μM) before the initiation of reactions. In BQ/Fe(III)/PMS process, BQ concentration quickly decreased to 93 μM and HQ concentration was not detectable after 1-min reaction (the first sampling point). With reaction time prolonging from 1 min to 60 min, BQ concentration slightly decreased to 87 μM. This

phenomenon was consistent with the CBZ degradation in the initial 1 min and the following reaction period (1–60 min). We also tracked the changes of HQ/BQ concentrations as functions of reaction time in HQ/Fe(III)/PMS system. The original 100 μM of HQ (20 μM was oxidized to BQ before PMS added) was barely detectable (<1.5 μM) after 1-min reaction (the first sampling point) and BQ concentration simultaneously increased to 88 μM (Fig. S7). Note that in the HQ/Fe(III) process without the presence of PMS, the reduction of Fe(III) by HQ proceeds through two one-electron-transfer steps via a semiquinone radical ($SQ^{\bullet-}$) as intermediate (Eqs. 3-4) (Duesteberg and Waite, 2007). BQ was generated slowly to reach the peak concentration and the conversion percentage was low (<10%) (Jiang et al., 2015). Whereas in the presence of PMS, the depletion of HQ and the formation of BQ were much faster (<1 min) (Figs. 3a-1). This is due to the faster transformation of HQ by $SO_4^{\bullet-}$ (Eq. 5), as the second-order reaction rate constant for HQ with $SO_4^{\bullet-}$ ($k > 1 \times 10^9\ M^{-1}s^{-1}$) (Anipsitakis et al., 2006) was much faster than that with Fe(III) ($k = 1 \times 10^3\ M^{-1}s^{-1}$) (Eq. 3) (Jiang et al., 2015). On the other hand, it is interesting to observe that only 13% of BQ was degraded in BQ/Fe(III)/PMS process after 60-min reaction, but theoretically, BQ should have a degradation percentage around 26% based on the second-order rate constant of BQ with $SO_4^{\bullet-}$ ($3.5 \times 10^8\ M^{-1}s^{-1}$) (Al-Suhybani and Hughes, 1986) and the $SO_4^{\bullet-}$ level (~2.03×10^{-13} M, obtained from Text S1). As such, some reaction pathways to convert the BQ oxidation products back to BQ may be involved, suggesting BQ as an electron shuttle in the system. More details were discussed in the next section.

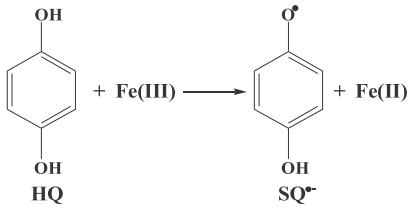

$k = 1 \times 10^3\ M^{-1}\ s^{-1}$

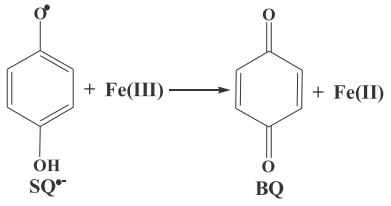

$k \leq 1 \times 10^5\ M^{-1}\ s^{-1}$

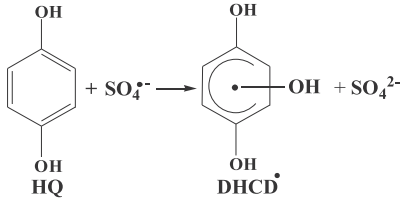

$k > 1 \times 10^9\ M^{-1}\ s^{-1}$

The generation of Fe(II) was confirmed in the BQ/Fe(III)/PMS process (Figs. 3a-2). Fe(II) concentration rapidly increased to 0.29 μM in 1 min and then maintained at this level during 15 min and then decreased gradually to 0.09 μM. The Fe(II) concentration was lower than that in BQ/Fe(III) system with the absence of PMS, which was around 0.8 μM during the reaction period of 1–30 min. Fe(II) is known to react with PMS to generate $SO_4^{\bullet-}$ (Eq. (1)) (Anipsitakis and Dionysiou, 2004), which can lead to the CBZ degradation. When ferrozine was added to the solution as a quencher for Fe(II), the CBZ degradation was greatly inhibited but still around 27% CBZ was degraded after 60-min reaction. This was mainly due to the BQ activation of PMS, which also led to CBZ degradation, though in a less extent (Fig. 1). When both ferrozine and BA were added as quenchers for Fe(II) and $SO_4^{\bullet-}$/$HO^{\bullet}$ respectively, negligible degradation of CBZ was observed. The results indicated the important role of Fe(II) formation in generating $SO_4^{\bullet-}$ and accelerating CBZ degradation.

Oxygen was involved in both the Fe(III)/Fe(II) and HQ/BQ redox reaction cycles and its role in CBZ degradation was thus evaluated. CBZ degradation in the solution purging with argon was faster than that in air-saturated condition (Fig. 3b-3). After 15-min reaction, 80% CBZ was degraded in argon-purged solution, higher than 44% degradation with oxygen present. BQ also had a faster degradation at the initial first min and gradually decreased to 75 μM over time. Regarding to Fe(II) concentration in argon-purged system, it rapidly increased to 0.32 μM in 1 min and then gradually decreased to 0.16 μM after 60 min, which was slightly higher than that with oxygen present. Thus, it seemed that more Fe(II) could react with PMS to generate $SO_4^{\bullet-}$ in argon-purged solution, which thus accelerated CBZ degradation. The inhibition of O_2 can also be attributed to the formation of superoxide anion radicals ($HO_2^{\bullet-}$), which can quench $SO_4^{\bullet-}$ quickly (Eqs. 6-7). In fact, the role of $HO_2^{\bullet-}$ in CBZ degradation was examined by adding SOD in the system with O_2 present. As shown in Fig. 3a-3, the degradation of CBZ increased from 20% to 32% in the first 1 min, which can be ascribed to SOD catalyzes the disproportion of $HO_2^{\bullet-}$ to H_2O_2 (Jiang et al., 2015).

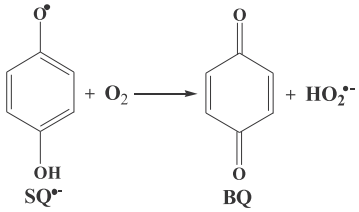

$k = 7 \times 10^2\ M^{-1}\ s^{-1}$

$$HO_2^{\bullet-} + SO_4^{\bullet-} \rightarrow SO_4^{2-} + H_2O \quad (7)$$

3.4. Reaction mechanisms

As mentioned above, three reactive species - $^1O_2$, $HO^{\bullet}$ and $SO_4^{\bullet-}$, were observed in the BQ/Fe(III)/PMS system, among which $SO_4^{\bullet-}$ was the dominant specie contributing to CBZ degradation. $SO_4^{\bullet-}$ was mainly generated from Fe(II) activation of PMS (Eq. (1)) and the formation of Fe(II) was the rate-limiting step. Fe(II) was formed from the reduction of Fe(III) by multiple reductants (e.g., HQ and $SQ^{\bullet-}$ (Eqs. 3-4)). The concentration of $SO_4^{\bullet-}$ was much higher in the beginning stage of the reaction (<1 min) in BQ/Fe(III)/PMS system than the later stage (1–60 min), due to the presence of trace amount HQ, which can rapidly reduce Fe(III) to Fe(II).

BQ is proposed to act as electron shuttle in the BQ/Fe(III)/PMS system. Along with CBZ, the residual BQ can be oxidized by $SO_4^{\bullet-}$. The initial product of BQ oxidation by $SO_4^{\bullet-}$ is benzoquinone-–OH–adduct radical, which then undergoes a very rapid, possibly water-assisted keto-enol tautomerization to give a 2,4-dihydroxyphenoxyl radical ($DHPO^{\bullet}$) (Eq. 8) (Al-Suhybani and Hughes, 1986; Nien Schuchmann et al., 1998). Subsequently, the 2,4-dihydroxyphenoxyl radical can be oxidized by another BQ to produce 2-hydroxy-1,4-benzoquinone (2-OH-BQ) and semiquinone radial ($SQ^{\bullet-}$) (Eq. 9) (Al-Suhybani and Hughes, 1986). $SQ^{\bullet-}$ can reduce Fe(III) to regenerate BQ again (Eq. 4). These reactions account for the lower rate of BQ decay observed in Section 3.3.

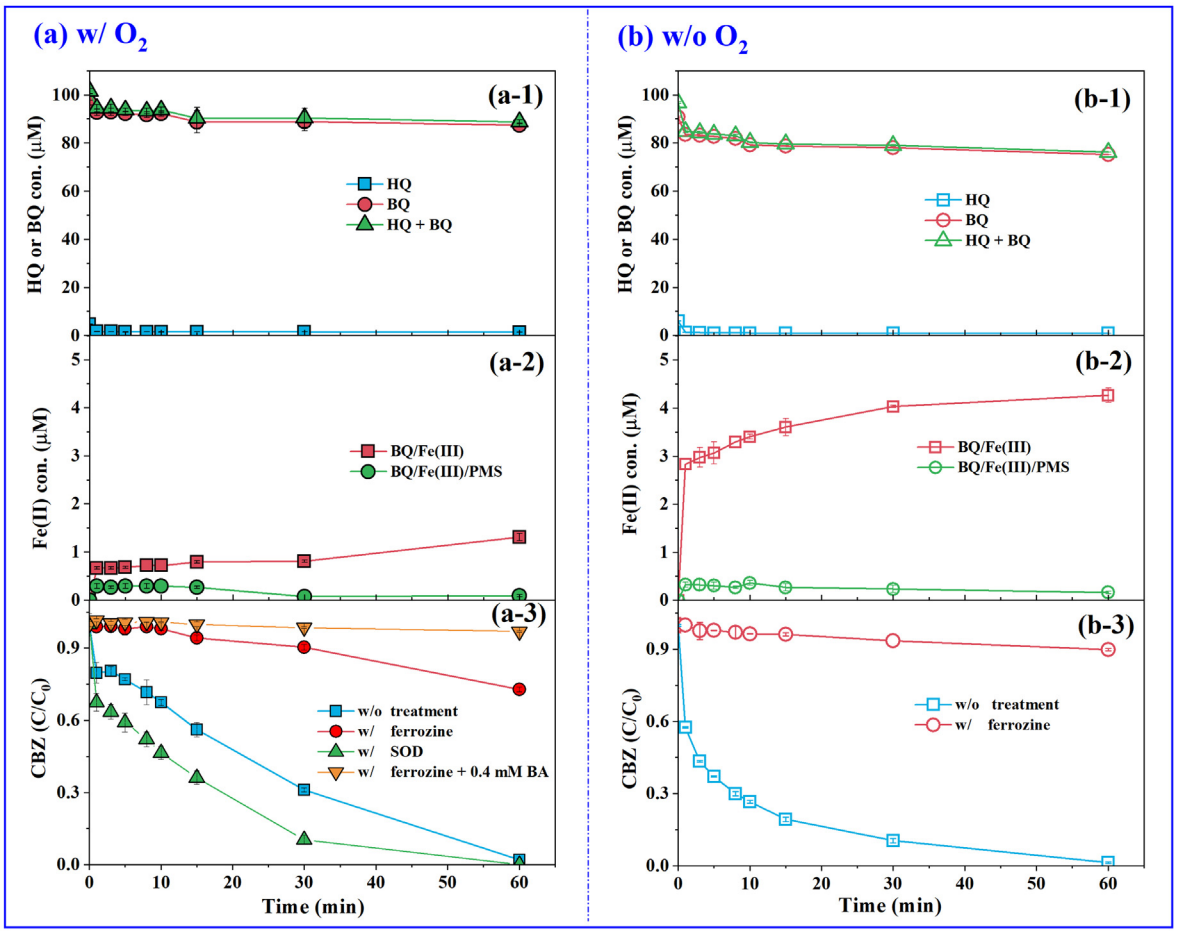

Fig. 3. BQ transformation, Fe(II) generation, and the effect of different quenchers on CBZ degradation in BQ/Fe(III)/PMS process: (a) in the presence of O_2 and (b) in the absence of O_2. (CBZ = 2 μM, Fe(III) = 0.05 mM, BQ = 0.1 mM, PMS = 0.5 mM, ferrozine = 0.15 mM).

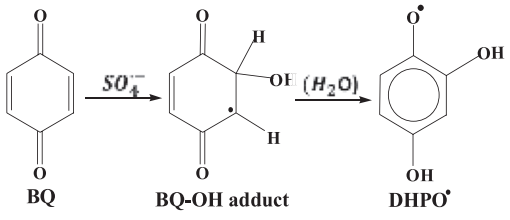

$k \cong 3.5 \times 10^{8}\ M^{-1}\ s^{-1}$

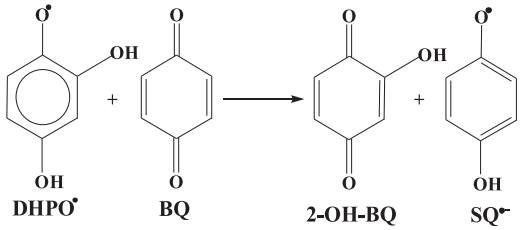

$k \leq 2.4 \times 10^{7}\ M^{-1}\ s^{-1}$

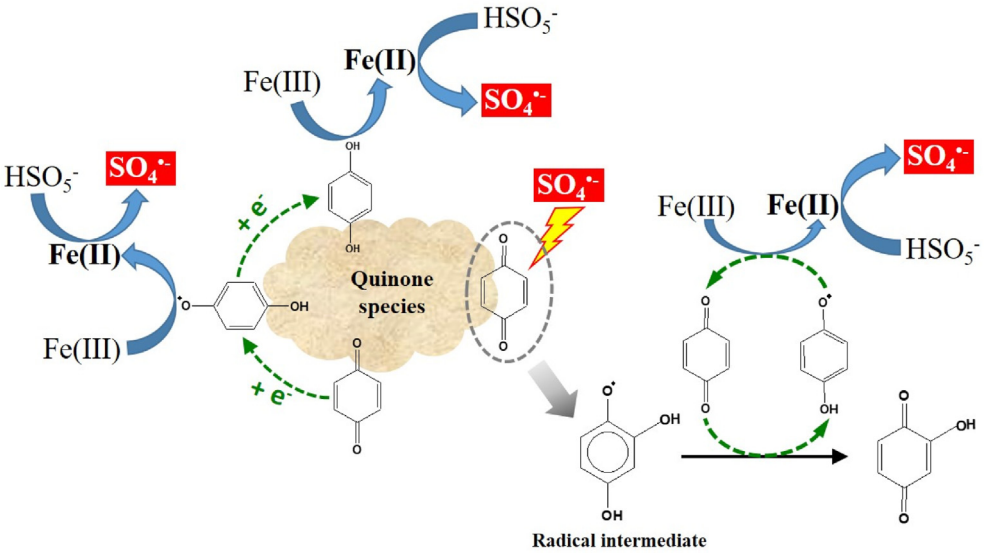

Scheme 1. Proposed mechanism of $SO_4^{\bullet-}$ generation in quinone/Fe(III)/PMS process.

Therefore, in BQ/Fe(III)/PMS system, BQ acts as an electron shuttle in transferring Fe(III) back to Fe(II) and Fe(II) activates PMS to produce $SO_4^{\bullet-}$ in promoting the degradation of micropollutants (e.g. CBZ). A reaction scheme is drawn and presented in Scheme 1.

3.5. PMS enhanced coagulation process for CBZ degradation in natural waters

NOM, bearing phenolic and quinone moieties, is ubiquitous in natural waters (Linkhorst et al., 2017). In order to verify if NOM can play a similar role as phenol/quinone, the degradation of CBZ was tracked following a coagulation/sedimentation process with $FeCl_3$ as the coagulant and with PMS amended in natural waters. Fig. 4a displays the CBZ abatement in PMS oxidation alone, Fe(III) coagulation alone, and PMS amended Fe(III) coagulation (abbreviated as Fe(III)/PMS coagulation) in Beijiang (SW1) and Pearl river samples (SW2). CBZ can be barely removed by either Fe(III) coagulation or PMS oxidation alone (<10%) in 120 min. However, when PMS was concomitantly added with Fe(III), the degradation percentages of CBZ reached 80% for Beijiang water and 50% for Pearl river water after coagulation/sedimentation in 120 min. Moreover, increasing PMS concentration enhanced CBZ degradation percentage in Beijiang water (Fig. 4b). When PMS increased from 0.2 to 1 mM, the corresponding CBZ degradation percentage increased from 15% to 81% after coagulation/sedimentation. In order to further highlight the important role of NOM in iron redox transformation and in PMS activation, CBZ was spiked to a solution containing SRFA (1–5 mg/L), an allochthonous aquatic NOM representative, to perform the Fe(III)/PMS coagulation process. As shown in Fig. 4c, the CBZ degradation increased rapidly in the solutions containing SRFA, Fe(III) and PMS. The degradation percentage of CBZ was 94% within 120 min in 1 mgC/L of SRFA-containing water, and rapidly increased to 100% after 60 min as SRFA increased to 2.5 mgC/L. Further increasing SRFA concentration from 2.5 mgC/L to 5 mgC/L could not lead to greater promotion on CBZ degradation, which might be due to the quenching effect of reactive species ($HO^{\bullet}$ and $SO_4^{\bullet-}$) by SRFA (Lutze et al., 2015; Xie et al., 2015). Again, TBA and methanol were respectively added to explore the role of $SO_4^{\bullet-}$ and $HO^{\bullet}$. Results showed that 30% of CBZ degradation was inhibited by TBA, while 60% was inhibited by methanol, suggesting that both $SO_4^{\bullet-}$ and $HO^{\bullet}$ contributed to CBZ degradation. The more pronounced $HO^{\bullet}$ contribution in SRFA solution than those of BQ and HQ systems may be due to the higher efficiency of $HO^{\bullet}$ formation from oxygenation of reduced SRFA and subsequently mediated Fenton reaction (Eqs. (10)–(12)) (Chen and Pignatello, 1997; Jiang et al., 2015; Page et al., 2012).

$$SRFA_{red} + O_2 \rightarrow SRFA_{ox} + HO_2^{\bullet} \quad (10)$$

$$HO_2^{\bullet} + HO_2^{\bullet} \rightarrow H_2O_2 + O_2 \quad k = 8.5 \times 10^5\ M^{-1}\ s^{-1} \quad (11)$$

$$H_2O_2 + Fe(II) \rightarrow OH^- + HO^{\bullet} + Fe(III) \quad k = 76\ M^{-1}\ s^{-1} \quad (12)$$

It should be noted that pH was not adjusted during the PMS enhanced coagulation/sedimentation process. In fact, the pH values deceased from 7.49 (the original pH of Beijiang water) to 6.82 in Fe(III) coagulation process and to 6.02 in PMS/Fe(III) coagulation processes (Table S4). The decreases in pH were due to the acidity of PMS (Wacławek et al., 2017). The results indicated that the efficient PMS activation can also be achieved in near-neutral natural water. On the one hand, NOM contains a wide range of redox active groups, such as quinone-hydroquinone moieties, which can generate Fe(II) via redox reactions for PMS activation (Daugherty et al., 2017). Thus, the reactions to degrade CBZ shared similarities as those in HQ/Fe(III)/PMS and BQ/Fe(III)/PMS systems. On the other hand, NOM consists of an extended network, in which some moieties (e.g. carboxyl and hydroxyl groups) can effectively complex with ferric irons to prevent their precipitation (Fujii et al., 2014), which is one of the prerequisites for Fe-mediated PMS activation. These aspects are beneficial for PMS activation. Undoubtedly, NOM also quenched $SO_4^{\bullet-}$ to reduce its levels (Lutze et al., 2015). Meanwhile, the reactions produced a wide range of products, which may also possibly activate PMS to generate $SO_4^{\bullet-}$. It should be noted that the enhanced coagulation process had little impact on the turbidity removal. After settling for 90 min, the residual turbidity and dissolved Fe in two surface water samples were both below the detection limits (<1 NTU for turbidity and 0.03 mg/L for dissolved Fe). Also, the concentrations of SO_4^{2-} were 216 mg/L for Beijiang water and 230 mg/L for Pearl River water, which were lower than the standard for drinking water quality (250 mg/L, GB 5749–2006). Note that the concentrations of TrOCs in source water are normally much lower than that used in this study (0.5 μM), thus

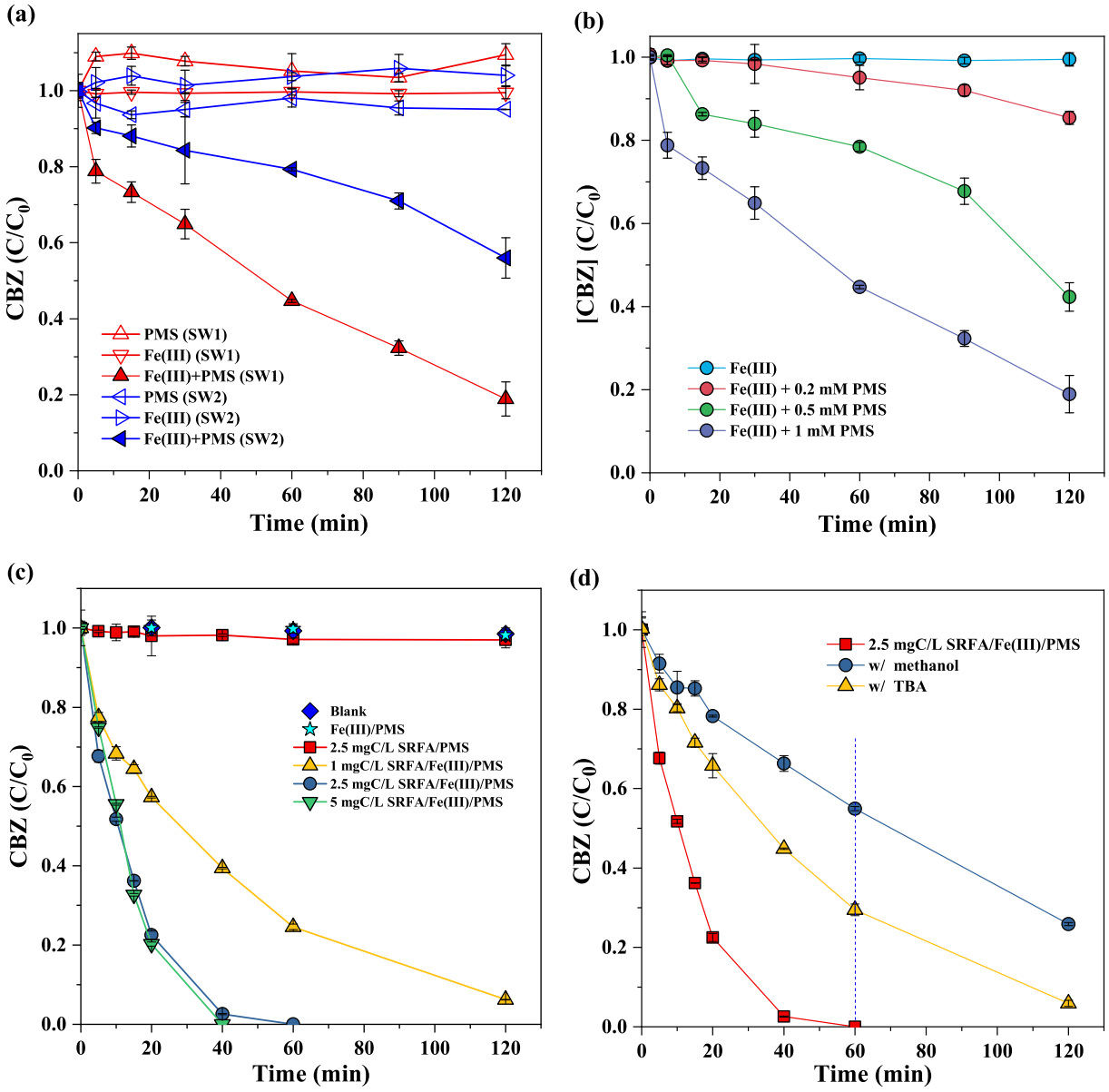

Fig. 4. (a) CBZ degradation by PMS-enhanced iron coagulation in different natural waters (SW1 and SW2 refer to Beijiang River and Pearl River waters, respectively). (CBZ = 0.5 μM, Fe(III) = 0.2 mM, PMS = 0–1 mM); (b) Effect of PMS dosage on CBZ degradation in SW1 water; (c) The degradation of CBZ by Fe(III)/PMS process in the presence or absence of SRFA. (CBZ = 1 μM, Fe(III) = 20 μM, PMS = 0.2 mM); (d) Effect of 10 mM methanol or TBA on CBZ degradation by Fe(III)/PMS process in SRFA-containing water.

a smaller quantity of PMS would be used to effectively degrade TrOCs. The PMS enhanced Fe(III) coagulation seems to be a promising process for TrOCs removal in water treatment. Especially for urgent water deterioration, upgrading the conventional coagulation process to an AOP mediated coagulation process can be effective to reduce the risks of TrOCs.

4. Conclusions

This study demonstrated that peroxomonosulfate (PMS) amended iron coagulation process can effectively degrade TrOCs including CBZ due to $SO_4^{\bullet-}$ generation in the system. The generation of Fe(II) was the rate limiting step for CBZ degradation and Fe(II) activation of PMS to generate $SO_4^{\bullet-}$ was the major mechanism leading to CBZ degradation. The Fe(III)/Fe(II) redox cycle was driven by HQ and BQ transformation and BQ served as the electron shuttle in the reaction system to accelerate the generation of Fe(II) and $SO_4^{\bullet-}$. NOM in natural waters containing quinone-hydroquinone moieties can also generate Fe(II) via redox reactions for PMS activation. The significant removal of CBZ in natural waters following the full treatment chain of PMS amended coagulation/flocculation/sedimentation proved the effectiveness of the proposed treatment method. Overall, this study provides new insights into the pathway of PMS activation and provides an efficient way to improve the common drinking water treatment process for TrOCs abatement. As NOM is a heterogeneous mixture and contains a wide range of redox-active functional groups, future studies should consider the impact of the nature of NOMs on the performance of the oxidation treatment system.

Declaration of competing interest

The authors declare that they have no known competing financial interests or personal relationships that could have

appeared to influence the work reported in this paper.

Acknowledgments

We thank the National Key Research and Development Program of China (2017YFE0133200), Guangdong Basic and Applied Basic Research Foundation (2019A1515012036), National Natural Science Foundation of China (21806193) and China Postdoctoral Science Foundation (2018M633226).

Appendix A. Supplementary data

Supplementary data to this article can be found online at https://doi.org/10.1016/j.watres.2020.116136.

References

Aeschbacher, M., Graf, C., Schwarzenbach, R.P., Sander, M., 2012. Antioxidant properties of humic substances. Environ. Sci. Technol. 46 (9), 4916–4925.
Ahmad, M., Teel, A.L., Watts, R.J., 2013. Mechanism of persulfate activation by phenols. Environ. Sci. Technol. 47 (11), 5864–5871.
Al-Suhybani, A.A., Hughes, G., 1986. Radiolysis of p-benzoquinone solutions. J. Radioanal. Nucl. Chem. 98 (1), 17–29.
Anipsitakis, G.P., Dionysiou, D.D., 2004. Radical generation by the interaction of transition metals with common oxidants. Environ. Sci. Technol. 38 (13), 3705–3712.
Anipsitakis, G.P., Dionysiou, D.D., Gonzalez, M.A., 2006. Cobalt-mediated activation of peroxymonosulfate and sulfate radical attack on phenolic compounds. Implications of chloride ions. Environ. Sci. Technol. 40 (3), 1000–1007.
Bruce, G.M., Pleus, R.C., Snyder, S.A., 2010. Toxicological relevance of pharmaceuticals in drinking water. Environ. Sci. Technol. 44 (14), 5619–5626.
Buxton, G.V., Greenstock, C.L., Helman, W.P., Ross, A.B., 1988. Critical review of rate constants for reactions of hydrated electrons, hydrogen atoms and hydroxyl radicals ($^{\bullet}OH/^{\bullet}O^{-}$) in aqueous solution. J. Phys. Chem. Ref. Data 17 (2), 513–886.
Chen, R., Pignatello, J.J., 1997. Role of quinone intermediates as electron shuttles in Fenton and photoassisted Fenton oxidations of aromatic compounds. Environ. Sci. Technol. 31 (8), 2399–2406.
Cheng, S., Lei, Y., Lei, X., Pan, Y., Lee, Y., Yang, X., 2020. Co-exposure degradation of purine derivatives in sulfate radical-mediated oxidation process. Environ. Sci. Technol. 54 (2), 1186–1195.
Cory, R.M., McKnight, D.M., 2005. Fluorescence spectroscopy reveals ubiquitous presence of oxidized and reduced quinones in dissolved organic matter. Environ. Sci. Technol. 39 (21), 8142–8149.
Daugherty, E.E., Gilbert, B., Nico, P.S., Borch, T., 2017. Complexation and redox buffering of iron(II) by dissolved organic matter. Environ. Sci. Technol. 51 (19), 11096–11104.
Duesteberg, C.K., Waite, T.D., 2007. Kinetic modeling of the oxidation of p-hydroxybenzoic acid by Fenton's reagent: implications of the role of quinones in the redox cycling of iron. Environ. Sci. Technol. 41 (11), 4103–4110.
Fang, G.D., Gao, J., Dionysiou, D.D., Liu, C., Zhou, D.M., 2013. Activation of persulfate by quinones: free radical reactions and Implication for the Degradation of PCBs. Environ. Sci. Technol. 47 (9), 4605–4611.
Fujii, M., Imaoka, A., Yoshimura, C., Waite, T.D., 2014. Effects of molecular composition of natural organic matter on ferric iron complexation at circumneutral pH. Environ. Sci. Technol. 48 (8), 4414–4424.
Gaffney, V.d.J., Almeida, C.M.M., Rodrigues, A., Ferreira, E., Benoliel, M.J., Cardoso, V.V., 2015. Occurrence of pharmaceuticals in a water supply system and related human health risk assessment. Water Res. 72, 199–208.
Garg, S., Jiang, C., Waite, T.D., 2015. Mechanistic insights into iron redox transformations in the presence of natural organic matter: impact of pH and light. Geochem. Cosmochim. Acta 165, 14–34.
Ghanbari, F., Moradi, M., 2017. Application of peroxymonosulfate and its activation methods for degradation of environmental organic pollutants: Review. Chem. Eng. J. 310, 41–62.
Huerta-Fontela, M., Galceran, M.T., Ventura, F., 2011. Occurrence and removal of pharmaceuticals and hormones through drinking water treatment. Water Res. 45 (3), 1432–1442.
Jiang, C., Garg, S., Waite, T.D., 2015. Hydroquinone-mediated redox cycling of iron and concomitant oxidation of hydroquinone in oxic waters under acidic conditions: comparison with iron-natural organic matter interactions. Environ. Sci. Technol. 49 (24), 14076–14084.
Kim, C., Ahn, J.Y., Kim, T.Y., Shin, W.S., Hwang, I., 2018. Activation of persulfate by nanosized zero-valent iron (NZVI): mechanisms and transformation products of NZVI. Environ. Sci. Technol. 52 (6), 3625–3633.
Lee, J., von Gunten, U., Kim, J.H., 2020. Persulfate-bsed advanced oxidation: critical assessment of opportunities and roadblocks. Environ. Sci. Technol. 54 (6), 3064–3081.
Li, H., Shan, C., Pan, B., 2018. Fe(III)-doped g-C_3N_4 mediated peroxymonosulfate activation for selective degradation of phenolic compounds via high-valent iron-oxo species. Environ. Sci. Technol. 52 (4), 2197–2205.
Linkhorst, A., Dittmar, T., Waska, H., 2017. Molecular fractionation of dissolved organic matter in a shallow subterranean estuary: the role of the iron curtain. Environ. Sci. Technol. 51 (3), 1312–1320.
Liu, N., Jin, X., Feng, C., Wang, Z., Wu, F., Johnson, A.C., Xiao, H., Hollert, H., Giesy, J.P., 2020. Ecological risk assessment of fifty pharmaceuticals and personal care products (PPCPs) in Chinese surface waters: a proposed multiple-level system. Environ. Int. 136, 105454.
Loraine, G.A., Pettigrove, M.E., 2006. Seasonal variations in concentrations of pharmaceuticals and personal care products in drinking water and reclaimed wastewater in southern California. Environ. Sci. Technol. 40 (3), 687–695.
Lutze, H.V., Bircher, S., Rapp, I., Kerlin, N., Bakkour, R., Geisler, M., von Sonntag, C., Schmidt, T.C., 2015. Degradation of chlorotriazine pesticides by sulfate radicals and the influence of organic matter. Environ. Sci. Technol. 49 (3), 1673–1680.
Matilainen, A., Vepsalainen, M., Sillanpaa, M., 2010. Natural organic matter removal by coagulation during drinking water treatment: a review. Adv. Colloid Interfac. 159 (2), 189–197.
Neta, P., Madhavan, V., Zemel, H., Fessenden, R.W., 1977. Rate constants and mechanism of reaction of sulfate radical anion with aromatic compounds. J. Am. Chem. Soc. 99 (1), 163–164.
Nien Schuchmann, M., Bothe, E., von Sonntag, J., von Sonntag, C., 1998. Reaction of OH radicals with benzoquinone in aqueous solutions. A pulse radiolysis study. J. Chem. Soc. Perk. T. 2 (4), 791–796.
Padhye, L.P., Yao, H., Kung'u, F.T., Huang, C.H., 2014. Year-long evaluation on the occurrence and fate of pharmaceuticals, personal care products, and endocrine disrupting chemicals in an urban drinking water treatment plant. Water Res. 51, 266–276.
Page, S.E., Sander, M., Arnold, W.A., McNeill, K., 2012. Hydroxyl radical formation upon oxidation of reduced humic acids by oxygen in the dark. Environ. Sci. Technol. 46 (3), 1590–1597.
Pan, T., Wang, Y., Yang, X., Huang, X.F., Qiu, R.L., 2020. Gallic acid accelerated BDE47 degradation in PMS/Fe(III) system: oxidation intermediates autocatalyzed redox cycling of iron. Chem. Eng. J. 384, 123248.
Song, Y., Buettner, G.R., 2010. Thermodynamic and kinetic considerations for the reaction of semiquinone radicals to form superoxide and hydrogen peroxide. Free Radic. Biol. Med. 49 (6), 919–962.
Stookey, L.L., 1970. Ferrozine-a new spectrophotometric reagent for iron. Anal. Chem. 42 (7), 779–781.
Sun, B., Ma, W., Wang, N., Xu, P., Zhang, L., Wang, B., Zhao, H., Lin, K.Y.A., Du, Y., 2019. Polyaniline: a new metal-free catalyst for peroxymonosulfate activation with highly efficient and durable removal of organic pollutants. Environ. Sci. Technol. 53 (16), 9771–9780.
Vik, E.A., Eikebrokk, B., 1988. Aquatic Humic Substances. American Chemical Society, pp. 385–408.
Wacławek, S., Grübel, K., Černík, M., 2015. Simple spectrophotometric determination of monopersulfate. Spectrochim. Acta A 149, 928–933.
Wacławek, S., Lutze, H.V., Grübel, K., Padil, V.V.T., Černík, M., Dionysiou, D.D., 2017. Chemistry of persulfates in water and wastewater treatment: a review. Chem. Eng. J. 330, 44–62.
Westerhoff, P., Yoon, Y., Snyder, S., Wert, E., 2005. Fate of endocrine-disruptor, pharmaceutical, and personal care product chemicals during simulated drinking water treatment processes. Environ. Sci. Technol. 39 (17), 6649–6663.
Xie, P., Ma, J., Liu, W., Zou, J., Yue, S., Li, X., Wiesner, M.R., Fang, J., 2015. Removal of 2-MIB and geosmin using UV/persulfate: contributions of hydroxyl and sulfate radicals. Water Res. 69, 223–233.
Zhang, Q.Q., Ying, G.G., Pan, C.G., Liu, Y.S., Zhao, J.L., 2015. Comprehensive evaluation of antibiotics emission and fate in the river basins of China: source analysis, multimedia modeling, and linkage to bacterial resistance. Environ. Sci. Technol. 49 (11), 6772–6782.
Zhou, Y., Jiang, J., Gao, Y., Ma, J., Pang, S.Y., Li, J., Lu, X.T., Yuan, L.P., 2015. Activation of peroxymonosulfate by benzoquinone: a novel nonradical oxidation process. Environ. Sci. Technol. 49 (21), 12941–12950.
Zhu, S., Li, X., Kang, J., Duan, X., Wang, S., 2019. Persulfate activation on crystallographic manganese oxides: mechanism of singlet oxygen evolution for nonradical selective degradation of aqueous contaminants. Environ. Sci. Technol. 53 (1), 307–315.
Zou, J., Ma, J., Chen, L., Li, X., Guan, Y., Xie, P., Pan, C., 2013. Rapid acceleration of ferrous iron/peroxymonosulfate oxidation of organic pollutants by promoting Fe(III)/Fe(II) cycle with hydroxylamine. Environ. Sci. Technol. 47 (20), 11685–11691.